

Geophysical Research Letters®



RESEARCH LETTER

10.1029/2024GL108829

Increased Summer Monsoon Rainfall Over Northwest India Caused by Hadley Cell Expansion and Indian Ocean Warming

Ligin Joseph¹ , Nikolaos Skliris¹, Dipanjan Dey^{1,2}, Robert Marsh¹, and Joël Hirschi³ 

¹School of Ocean and Earth Science, University of Southampton, Southampton, UK, ²School of Earth, Ocean and Climate Sciences, Indian Institute of Technology Bhubaneswar, Argul, Khordha, India, ³Marine Systems Modelling, National Oceanography Centre, Southampton, UK

Key Points:

- Large increase in summer monsoon precipitation over Northwest India
- The strengthening of the monsoon winds and the Indian Ocean warming drives increasing evaporation
- Poleward shift and expansion of high-pressure belts and the Indian Ocean warming are responsible for the strengthening of winds

Supporting Information:

Supporting Information may be found in the online version of this article.

Correspondence to:

L. Joseph,
l.joseph@soton.ac.uk

Citation:

Joseph, L., Skliris, N., Dey, D., Marsh, R., & Hirschi, J. (2024). Increased summer monsoon rainfall over Northwest India caused by Hadley cell expansion and Indian Ocean warming. *Geophysical Research Letters*, 51, e2024GL108829. <https://doi.org/10.1029/2024GL108829>

Received 24 FEB 2024

Accepted 6 AUG 2024

Abstract From 1979 to 2022, the summer monsoon precipitation has increased by a substantial 40% over Northwest India compared to the 1980s. This wetting trend aligns with the future projections of the Coupled Model Intercomparison Project 6 (CMIP6). The observationally constrained reanalysis data indicates that significant sea surface warming in the western equatorial Indian Ocean and the Arabian Sea is likely driving this increase in rainfall by enhancing the cross-equatorial monsoonal flow and associated evaporation. We demonstrate that the strengthening of the cross-equatorial monsoon winds is due to the rapid warming of the Indian Ocean and the enhanced Pacific Ocean trade winds, which result from the poleward shift and expansion of the Hadley cell. These strengthened winds boost the latent heat flux (evaporation), leading to increased moisture transport to Northwest India.

Plain Language Summary From 1979 to 2022, the summer monsoon precipitation has increased by a substantial 40% over Northwest India compared to the 1980s. The analysis suggests that a noticeable warming of the sea surface in the western equatorial Indian Ocean and the Arabian Sea could be causing this increase in rainfall. This warming strengthens the winds crossing the equator in the Indian Ocean and increases evaporation. The study also shows that the monsoon winds are strengthened due to the rapid warming of the Indian Ocean and the enhanced Pacific Ocean trade winds. These stronger winds cause more evaporation, which means more moisture is carried from the ocean to the land, leading to increased monsoon rainfall.

1. Introduction

India receives approximately 80% of its total rainfall during the Indian Summer Monsoon (ISM) season from June through September (JJAS). Billions of people depend on monsoon rainfall for food, water security, and electricity. The timing and intensity of ISM rainfall play a significant role in shaping the country's economy (Gadgil & Gadgil, 2006; Gadgil & Gadgil, 2006; Prasanna, 2014; Prasanna, 2014; Saha et al., 1979; Saha et al., 1979). Extreme rainfall events have tripled in India since 1950, resulting in devastating flooding events that cost the country about 3 billion dollars annually (Roxy et al., 2017). Therefore, projecting and forecasting the ISM rainfall variability in a warming climate is crucial for sustainable development, water resource management, and policymaking. However, ISM rainfall exhibits temporal variability spanning intra-seasonal to multi-decadal time scales (See Hrudya et al., 2021 for a recent review), and it involves complex interactions between different factors (Rao et al., 2019).

The differential heating between the land and the sea and the northward migration of the Inter Tropical Convergence Zone (ITCZ) drive the south-westerly winds, which carry moisture from the ocean toward the land, resulting in ISM rainfall (Gadgil, 2018; Gadgil, 2018; Roxy et al., 2015; Roxy et al., 2015). Evaporation over the central and south Indian Ocean is the major contributor to the ISM rainfall, followed by contributions from local recycling, the Arabian Sea, remote sources, and the Bay of Bengal (Dey & Döös, 2021). The Indian Ocean is warming rapidly compared to other tropical oceanic regions. Observations indicate a basin-scale warming of the Indian Ocean that is more prominent in the west equatorial region and the Arabian Sea (Rao et al., 2012; Roxy et al., 2014; Sharma et al., 2023; Swapna et al., 2014). This sea surface warming has the potential to increase evaporation, making more moisture available in the atmosphere along the typical moisture transport pathway over the Indian Ocean, which feeds ISM rainfall (Dey & Döös, 2021; Skliris et al., 2022).

© 2024. The Author(s).

This is an open access article under the terms of the [Creative Commons Attribution License](https://creativecommons.org/licenses/by/4.0/), which permits use, distribution and reproduction in any medium, provided the original work is properly cited.

Several studies have shown that the frequency and intensity of ISM rainfall are increasing in a warming climate (Bhowmick et al., 2021; Hari et al., 2020; Katzenberger et al., 2021; Rai & Raveh-Rubin, 2023; B. Wang et al., 2013). For instance, Katzenberger et al. (2021) projected an increase of 5% in ISM rainfall per degree of global warming in the late 21st Century, and Wang et al. (2013) showed that the northern hemisphere summer monsoon is intensifying due to mega-El Niño/Southern Oscillation and a hemispherical asymmetric response to global warming. Furthermore, the climate model simulations of Coupled Model Intercomparison Project 6 (CMIP6) robustly indicate a strengthening of the ISM rainfall in a warming climate. However, some studies have shown that, on the contrary, the ISM is weakening due to the reduced land-sea thermal gradient caused by the rapid Indian Ocean warming (Roxy et al., 2014, 2015; Swapna et al., 2014; Wang et al., 2022; R. K. Yadav & Roxy, 2019).

Considering these contrasting results, further analysis of the recent changes in ISM rainfall is needed. Furthermore, most ISM research is focused on central and northeast India, whereas only a few recent studies have focused on the monsoon trends in the western region. Rajesh and Goswami (2023) showed that the mean rainfall over northwest India and Pakistan has increased by 10%–50% during 1901–2015 and is expected to increase by 50%–200% under the moderate greenhouse gas scenarios. Li et al. (2023) showed that the springtime warming in the Middle East enhances the summer monsoon over northwestern India and Pakistan by strengthening the meridional sea level pressure gradient between the Middle East and the southern Arabian Sea, and driving the changes in the low-level jet. Mahendra et al. (2024) showed ISM rainfall over northwestern India is increasing and it is associated with the Silk Road Pattern phase change in the 1990s. R. Yadav (2024) showed that the ISM rainfall has shifted westward due to south-central equatorial Indian Ocean warming which increases the in-situ convection and Hadley cell subsidence branches over South Africa and eastern Europe. R. Yadav (2024) further showed that the anomalous subsidence over east Europe increases the adiabatic warming, which excites a Rossby wave toward central Asia, redirecting the migratory mid-latitude troughs to penetrate northwest India, shifting ISM rainfall westward. Based on these studies, it is clear that the ISM precipitation over the northwest Indian region is increasing significantly; however, the effect of the large-scale wind circulation changes on the moisture transport and precipitation trend is still unexplored.

The objectives of this study are thus to investigate the precipitation trend over Northwest India using state-of-the-art reanalysis and observational data sets, focusing on the possible role played by large-scale changes in wind patterns. This paper is organized as follows. The data set and the methods used in this study are described in Section 2. In Section 3, the main results are documented. The final section summarizes the results of the present work and provides concluding remarks.

2. Data and Methods

2.1. Observational and Reanalysis Data Sets

The data sets used in this study include in-situ, remote sensing, and atmospheric reanalysis data. The precipitation data set is obtained from the Indian Meteorological Department (IMD), which is a high spatial resolution daily gridded data set ($0.25 \times 0.25^\circ$) (Pai et al., 2014). The monthly data sets for winds, specific humidity, Mean Sea Level Pressure (MSLP), land evaporation, and vertically integrated water vapor flux (vertically integrated moisture transport hereafter) are obtained from ERA5 reanalysis (Hersbach et al., 2020). Monthly Sea Surface Temperature (SST) data are obtained from the HadISST1 data set provided by the Met Office Hadley Center (Rayner et al., 2003). The oceanic evaporation data are obtained from OAflux (Yu & Weller, 2007). The time series of Niño 3.4 and the Southern Annular Mode (SAM) index are obtained from the Physical Sciences Laboratory (PSL) and the Climate Data Guide (CDG). All analyses are conducted from 1979 to 2022. The data file for CMIP6 analysis is downloaded from the IPCC WGI Interactive Atlas (Iturbide et al., 2021).

2.2. Hadley Cell Extent and Removing ENSO Effect

The poleward extent of the Hadley cell is calculated as the latitude at which the zonal mean of the zonal wind at 925 hPa is closest to zero. Similar results with a correlation of ~ 0.8 are derived using a time series of the latitude at which the 500 hPa mean meridional stream function crosses zero poleward of its tropical extremum in the southern hemisphere. This suggests that our results are not dependent on the metrics we choose for the Hadley cell extent.

Numerous studies have documented the impact of El Niño-Southern Oscillation (ENSO) on the Hadley circulation and have shown that the circulation expands during La Niña and contracts during El Niño (Lyon & Barnston, 2005). The effect of ENSO can be removed from an observed field ($A(x,t)$) using the approach defined by (Schmidt & Grise, 2017). At each location x , let $R(x)$ be the slope of the linear regression of $A(x,t)$ to the Niño 3.4 index ($N(t)$). Then, the ENSO-congruent time series at each location is $R(x)N(t)$, and the residual time series, after ENSO removal, is as follows:

$$B(x,t) = A(x,t) - R(x)N(t) \quad (1)$$

The fields are detrended before computing the regression analysis.

2.3. Percentage Change, Trend and Statistical Significance Test

The percentage change in a parameter is calculated as the trend over 44 years divided by the mean during 1979–1988. The trend is calculated using the ordinary least squares (OLS) linear regression method. The statistical significance of the trend is assessed using the two-tailed t -test, with the null hypothesis that there is no trend and an alternative hypothesis that the trend is non-zero. This approach detects significant trends in both directions, regardless of whether the trend is increasing or decreasing.

3. Results

In Section 3.1, we first examine trends in regional precipitation and the associated atmospheric moisture transport, partitioning this between trends in winds and specific humidity. In Section 3.2, we further link these ISM changes to atmospheric circulation across the Indo-Pacific region, evident in 850-hPa wind trends, and attribute the drivers of these trends to evolving patterns of sea level pressure.

3.1. Trends in Precipitation and Moisture Transport

The ISM rainfall is characterized by large regional differences with maximum JJAS mean precipitation over northeast India and Western Ghats and minimum over northwest India (supplementary Figure S1 in Supporting Information S1). The ISM precipitation trend during 1979–2022 shows increased precipitation over northwest India, modest increases in central and southern parts of the country and decreasing precipitation in northeast India (Figure 1a). Northwest India is a semi-arid region, and an increase in precipitation could impact the population and would require better policymaking. Therefore, in this study, we focus on understanding the physical mechanisms driving this trend.

The northwest Indian region (NWI; black box in Figure 1a; 21°N–28°N; 69°E–77°E) typically receives a mean rainfall (evaporation) of ~4.07 (2.17) mm/day during the summer monsoon period. However, the region experienced a precipitation (evaporation) increase of ~40% (10%) compared to the 1979–1988 period. The percentage change in the frequency of daily rainfall during JJAS in the last decade (2013–2022) compared to the first decade (1979–1988) over NWI is shown in Figure 1b (actual values of frequency for the mentioned time periods are shown in supplementary Figure S3 in Supporting Information S1). The frequency of rainfall events has notably increased throughout the distribution, suggesting that the mean state and the number of extreme events have increased over this region.

If we assume that the observed precipitation trend over NWI is linked to global warming, then we should expect to note the same trend in the CMIP6 model projections. To test this, the percentage change in rainfall between 2081–2100 and 1850–1900 is plotted in Figure 1c. The CMIP6 projections show a substantial increase in JJAS precipitation with a pronounced rise over the NWI under the highest greenhouse gas emission scenario (SSP5–8.5) (Figure 1c), suggesting a possible role of anthropogenic warming in the wet trend. The trends in precipitation and evaporation over NWI suggest that the rise in precipitation cannot be solely attributed to local evaporation, indicating an influx of external moisture. Therefore, the vertically integrated moisture transport budget is computed and shown in Figure 1d. The mean vertically integrated moisture budget analysis (blue arrows; Figure 1d) suggests that the moisture usually enters from the western and southern boundary and exits through the eastern and northern boundary in the NWI region. Additionally, a moisture budget trend analysis (red arrows; Figure 1d) revealed an overall moisture convergence, which is driven by ~68% increased moisture entering from the Arabian Sea concomitant with strongly reduced outgoing moisture transport through the eastern (~38%) and

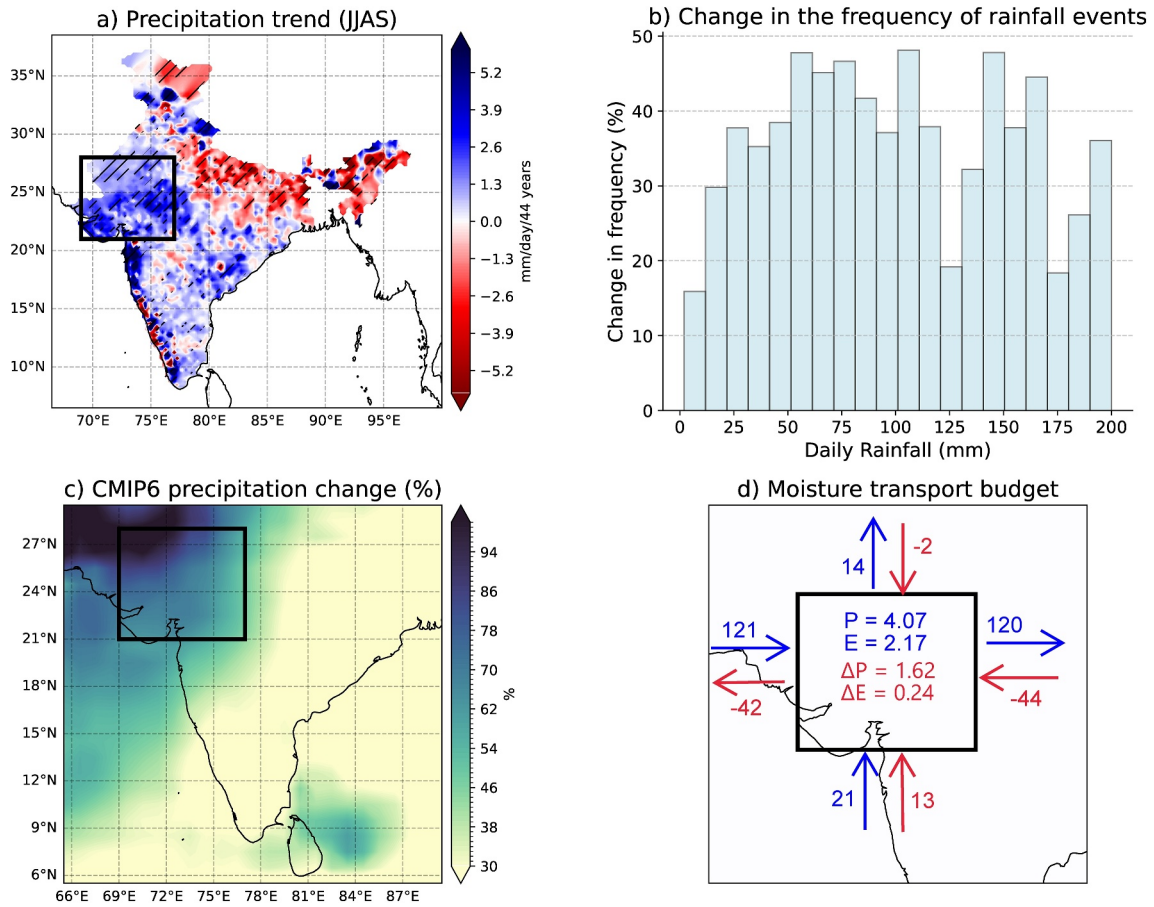


Figure 1. (a) Trend in JJAS precipitation (mm/day/44 years) from IMD data set during 1979–2022. The hashed regions show values that are significant at the 95% confidence level. (b) The percentage change (2013–2022 compared to 1979–1988) in the frequency of daily rainfall (mm) in JJAS over Northwest India (black box; 21°N–28°N; 69°E–77°E). (c) JJAS precipitation long-term (2081–2100) change relative to 1850–1900 in SSP5-8.5 emissions scenario from the CMIP6 ensemble (%). (d) JJAS vertically integrated moisture transport budget analysis over 1979–2022 from ERA5. The direction and value of the mean over 1979–1988 ($\text{kg m}^{-1} \text{s}^{-1}$) are shown in blue, and trends ($\text{kg m}^{-1} \text{s}^{-1}$ over 44 years) are shown in red. The mean values over 1979–1988 (mm/day) of precipitation P and evaporation E , along with their total change (mm/day over 44 years) ΔP and ΔE over the study region are shown inside the box. Note that the moisture transport and precipitation (evaporation) units are different.

northern ($\sim 12\%$) boundaries compared to the 1979–1988 mean (Figure 1d). Therefore, moisture entering through the Arabian Sea is vital in driving the rainfall variability over NWI.

The spatial trend of JJAS vertically integrated moisture transport is shown in Figure 2a, which confirms that more moisture is transported from the ocean toward the NWI landmass. It further shows an extensive increase in moisture transport along the tropical Indian and Pacific Oceans. The increasing trend can occur due to increased wind speed and/or increased moisture in the atmosphere. It is well documented in the literature that most of the moisture available in the atmosphere is concentrated at lower levels (Dey & Döös, 2019). Further, the 850-hPa level, which is at an altitude of about 1.5 km, is often used to study the monsoon circulation (Gadgil, 2018). Therefore, we calculated the moisture transport at 850 hPa and its trend is shown in Figure 2b. To analyze the relative contribution of wind and specific humidity to the trend in moisture transport at 850 hPa, the following approximate decomposition is used:

$$\frac{d(Uq)}{dt} = \bar{U} \frac{dq}{dt} + \bar{q} \frac{dU}{dt} + \text{Residual} \quad (2)$$

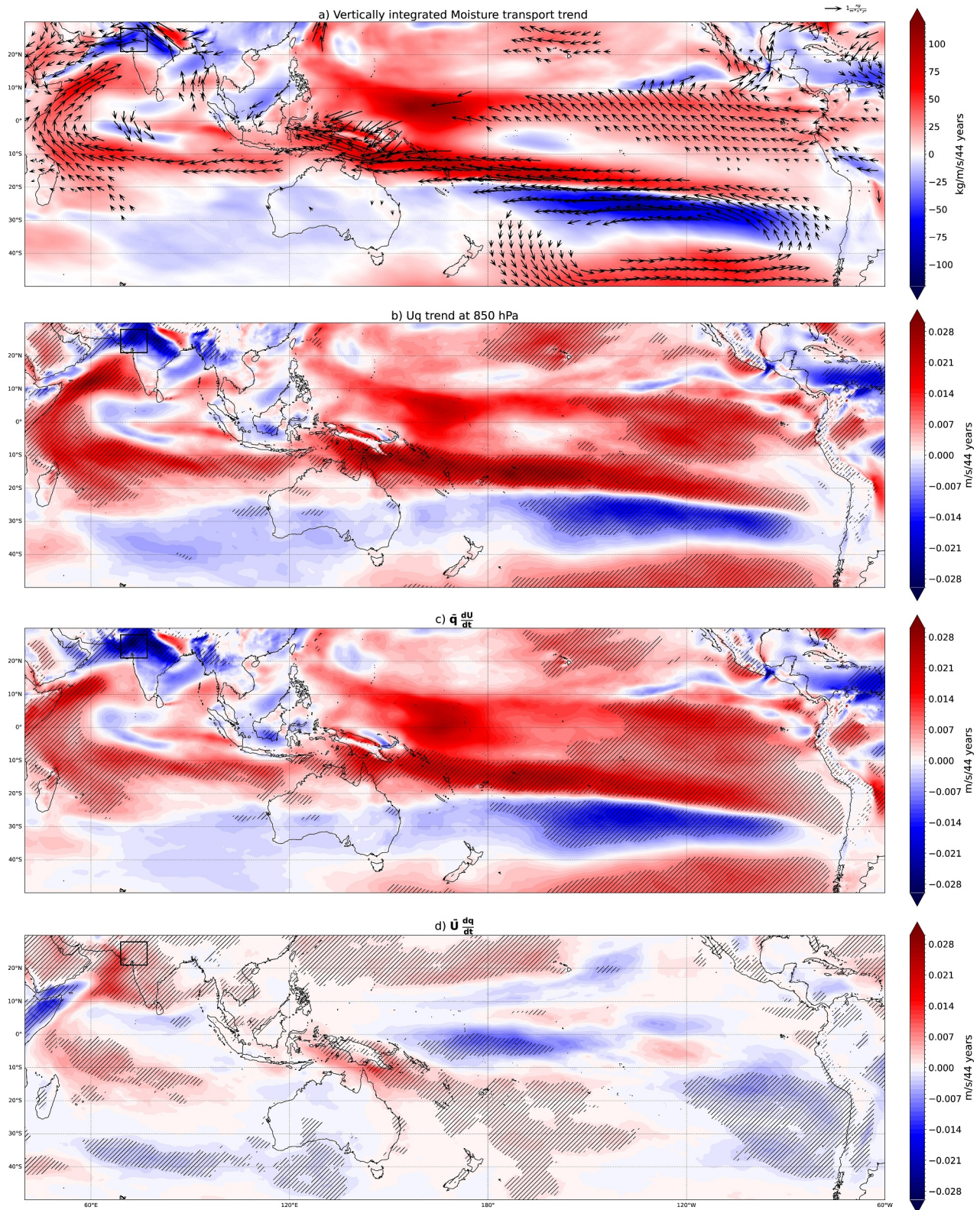


Figure 2.

here \bar{U} and \bar{q} are the means and $\frac{dU}{dt}$ and $\frac{dq}{dt}$ are the trends of wind speed and specific humidity at 850 hPa. The terms $\bar{q}\frac{dU}{dt}$ and $\bar{U}\frac{dq}{dt}$ are the contributions of wind speed change and specific humidity change, respectively, which drive the moisture transport trend.

The spatial plots of $\bar{q}\frac{dU}{dt}$ and $\bar{U}\frac{dq}{dt}$ are shown in Figures 2c and 2d which reveal that the moisture transport trend is attributed to changes in the wind pattern with a relatively lower but significant contribution from the changes in specific humidity, particularly over the Arabian Sea. The increased moisture transport trend across the southern boundary of NWI is found to be associated with the broad-scale wind trends over the Indian Ocean and humidity trends over the Arabian Sea (Figures 2c and 2d). Therefore, it is essential to analyze the changes in the wind pattern.

3.2. 850 hPa Wind Trends and Drivers

The low-level 850-hPa wind trend suggests an overall strengthening of the cross-equatorial monsoon winds and the Pacific Ocean trade winds (Figure 3a). The strengthening of the wind drives an increase in oceanic evaporation which results in more moisture being available in the atmosphere (Figure 3b). Apart from the wind speed, the SST can also impact evaporation by modifying the moisture gradient. The SST trend pattern indicates a basin-scale warming of the Indian Ocean that is more prominent in the west equatorial region and the Arabian Sea (Figure 3c). It is expected that the evaporation increases with an increase in SST as a thermodynamic response; however, the close similarity between the wind speed (Figure 3a) and the evaporation rate (Figure 3b) trends over the Indian Ocean reveals that the dynamical process (wind speed) is also vital in driving the evaporation over this region. Furthermore, the strengthened monsoon winds will transport more moisture from the ocean toward the NWI landmass, and the weakening of the wind over north India will reduce the moisture outflow, resulting in an overall convergence of moisture over this region. Therefore, it is essential to study the physical mechanisms driving these wind trend patterns.

The trend analysis of MSLP shows that the major high-pressure belts over the Indian and Pacific Oceans in the southern hemisphere have expanded and shifted poleward (Figure 4a). Previous studies have shown that the expansion and shift of high-pressure zones are attributed to Hadley cell expansion (Schmidt & Grise, 2017). To filter out the MSLP trends associated with the Hadley cell expansion, the ENSO effect from the MSLP is removed and then regressed onto the southern hemisphere Hadley cell extent time series (Section 2.2) (Figure 4b). The high significant positive regression coefficient over the Pacific Ocean signifies that the expansion of the Hadley cell resulted in an increased MSLP over this region, and this expansion is independent of ENSO.

This result agrees with numerous observational studies that show that the Hadley cell has been expanding poleward over the last few decades (Birner et al., 2014; D'Agostino et al., 2017; Hu & Fu, 2007; Lu et al., 2007; Lucas et al., 2014; Schmidt & Grise, 2017; Staten et al., 2019; Xian et al., 2021). Multiple factors are responsible for this expansion, including increasing greenhouse gases, stratospheric ozone depletion, and anthropogenic aerosols Lucas et al. (2014). Showed that this expansion is caused by an increase in the subtropical static stability, pushing the baroclinic instability zone poleward and, hence, the outer boundary of the Hadley cell. Numerous climate models have projected this poleward shift and expansion, with a 2–3 times more pronounced change in the southern hemisphere (Grise & Davis, 2020).

The poleward shift in the high-pressure zone over the southeast Pacific strengthens the trade winds, creating an anticyclonic motion around the increased MSLP over this region. This strengthening of the easterlies might result in the cooling of SST along the west coast of South America and far into the eastern Pacific through Ekman pumping and latent heat loss (Figure 3c), which can further increase the MSLP (Figure 4a) and acts as positive feedback in strengthening the southern hemisphere trade winds. Furthermore, a broad-scale decrease of MSLP is observed over the Indian Ocean (Figure 4a), with a significant decline in the west equatorial region, which is attributed to rapid Indian Ocean warming.

Figure 2. (a) Trend in JJAS vertically integrated moisture transport (colors—magnitude; $\text{kg m}^{-1}\text{s}^{-1}/44$ years). The arrows are plotted only if at least a component of the transport is statistically significant at the 95% confidence level. (b) Trend in JJAS moisture transport at 850 hPa ($\text{m s}^{-1}/44$ years). (c) JJAS mean of the specific humidity multiplied by the wind speed trend at 850 hPa ($\text{m s}^{-1}/44$ years). This map highlights the contribution of the wind change to moisture transport change. (d) JJAS mean wind speed multiplied by the trend in specific humidity at 850 hPa ($\text{m s}^{-1}/44$ years). This map highlights the contribution of the specific humidity change to the moisture transport change. The hashed regions indicate values that are significant at the 95% confidence level. All data sets used here are from ERA5.

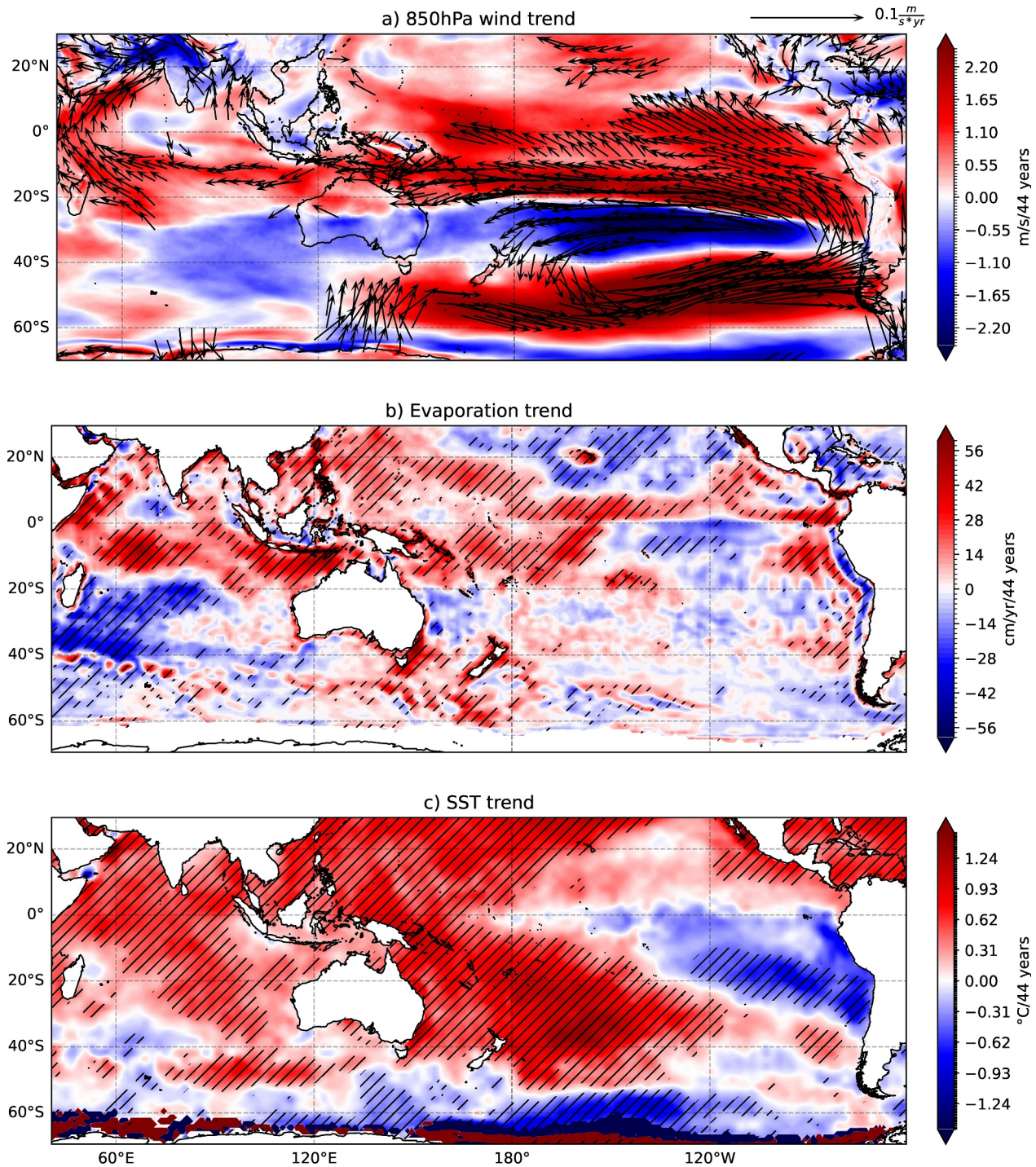


Figure 3. (a) Trend in JJAS 850 hPa wind (colors –speed ($\text{m s}^{-1}/44$ years)) from ERA5. The arrows are plotted only if at least a component of the wind is statistically significant at the 95% confidence level. (b) Trend in JJAS oceanic evaporation rate ($\text{cm ann}^{-1}/44$ years) from Oaflux. (c) Trend in JJAS SST ($^{\circ}\text{C}/44$ years) from HadISST1. The hashed regions indicate values that are significant at the 95% confidence level.

These MSLP trends induce a zonal pressure gradient with increased MSLP over the eastern Pacific and reduced MSLP over the Indian Ocean, which extends the strengthened trade winds from the Pacific toward the Indian Ocean. Further, the poleward shift and expansion of high pressure over the Mascarene High, along with the decrease in MSLP over the equatorial Indian Ocean, induces a meridional pressure gradient, which further

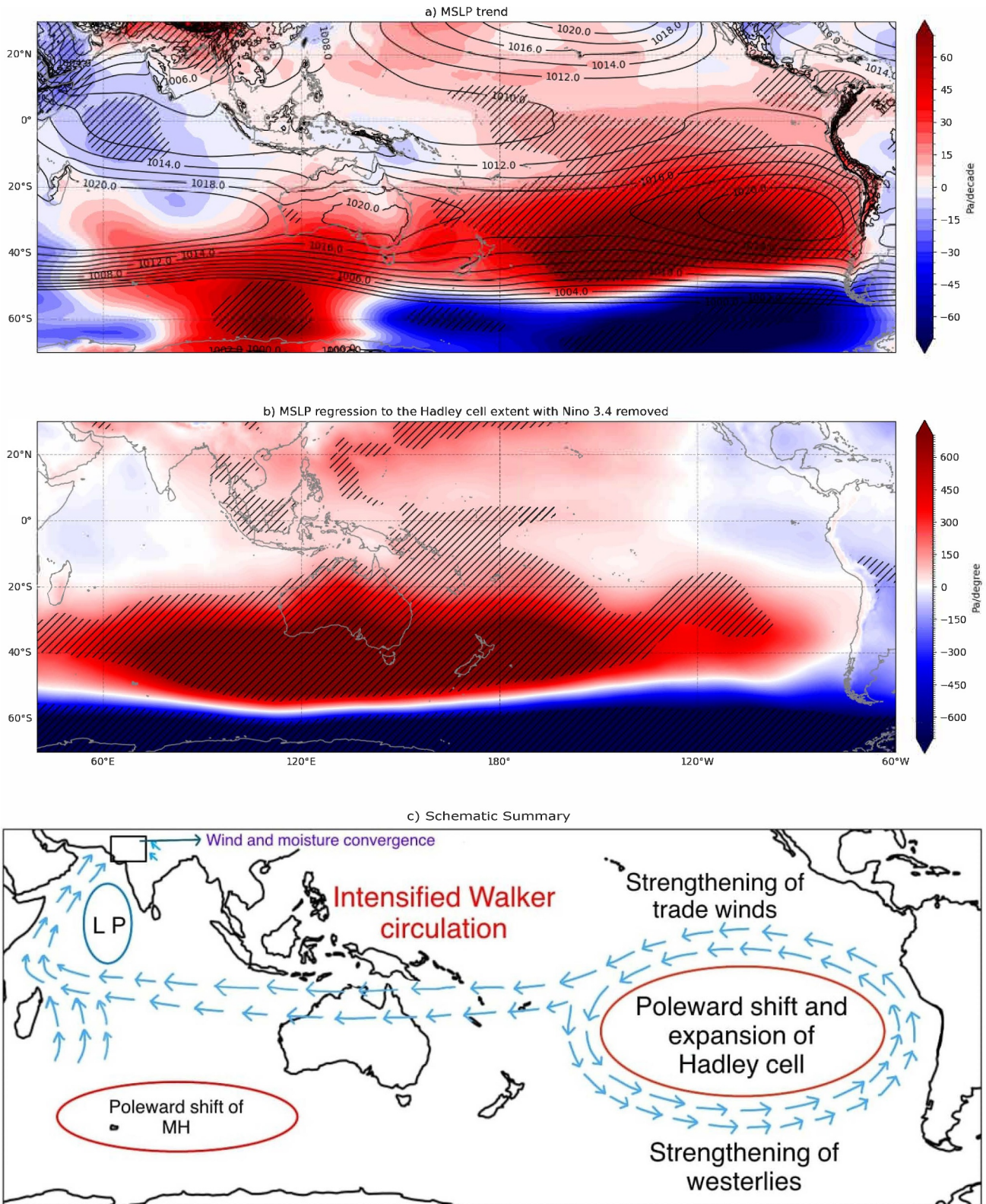


Figure 4. (a) Trend in JJAS MSLP (Pa/decade) from ERA5. JJAS mean of MSLP is plotted as contours (hPa). (b) Regression of detrended and ENSO removed JJAS MSLP onto the Hadley cell extent in the southern hemisphere (see Section 2.3). The hashed regions indicate values that are significant at the 90% confidence level. (c) A schematic summary of the study. LP stands for Low-Pressure and MH stands for Mascarene High.

strengthens the cross-equatorial monsoon winds. Therefore, these wind trend patterns result in an overall strengthening of moisture convergence over the NWI, hence substantially increasing rainfall (i.e., by ~40%) over this region during 1979–2022.

4. Discussion and Concluding Remarks

This study shows that the ISM rainfall over the NWI has increased by ~40% during 1979–2022. This precipitation increase is found to be driven by an enhancement of cross-equatorial monsoon winds, which increases evaporation over the Indian Ocean and transports more moisture from the Arabian Sea to NWI. It is further shown that the strengthening of the cross-equatorial monsoon winds is due to the rapid warming of the Indian Ocean and the enhanced Pacific Ocean trade winds. The strengthening of the southern hemisphere trade winds over the eastern Pacific is attributed to the shift and poleward expansion of the Hadley cell, whereas the strengthening along the western Pacific and Indian Ocean is due to the Indian Ocean warming. These wind patterns result in overall moisture convergence over Northwest India, with more moisture imported from the ocean and less exported, resulting in increased rainfall. A schematic summary is shown in Figure 4c.

The MSLP trend pattern in the Pacific resembles the positive phase of the Southern Annular Mode (SAM) (Fogt & Marshall, 2020; Fogt & Marshall, 2020; Fogt & Marshall, 2020). It is well documented in the literature that the positive SAM is associated with stronger than average westerlies over the mid-high latitudes (50–70S) and weaker westerlies in the mid-latitudes (30–0S) (Fogt & Marshall, 2020). The time series of the SAM index for JJAS calculated as the zonal pressure difference between the latitudes of 40 and 65S is shown in Figure S5 in Supporting Information S1. The frequency of positive SAM events has increased during the last decade. Therefore, it is plausible that these trends have an impact on the MSLP and 850-hPa wind trends. However, the regression of the SAM index onto the ENSO-removed MSLP could not explain the significant positive MSLP trend seen over the eastern Pacific (Figure S6 in Supporting Information S1). The poleward shift in the Hadley cell might explain the increasing frequency of positive SAM events; however, more research needs to be done to confirm this.

Furthermore, the strengthened trade winds have the potential to lower SST along the southeastern Pacific Ocean via Ekman pumping and latent heat loss, further intensifying the MSLP gradient and acting as possible positive feedback. Surface cooling across the tropical eastern Pacific is indicative of a La-Nina-type SST pattern. During the last decade, there were more prolonged La Nina than El-Niño events, which may account for some of the SST trend patterns (supplementary Figure S7 in Supporting Information S1) (Skliris et al., 2022). However, plotting the SST and MSLP trends after removing the ENSO effects shows similar results, and hence, it confirms that these trends are largely independent of ENSO.

Although the moisture availability in the atmosphere is expected to increase under global warming, future changes in the precipitation pattern over India will be strongly dependent on the changing monsoon atmospheric circulation, as evidenced in our results for the recent historical period. The wind pattern, in particular, will strongly control how much of the increased moisture originating from the ocean in the future will be transported toward the Indian landmass to feed local precipitation. Recent and future warming of the Indian Ocean is complicit in the changing ISM. The CMIP6 model projections show continued warming of the Indian Ocean and expansion of the Hadley cell in all future scenarios. This has the potential to intensify the MSLP gradient and, hence, can strengthen the trade winds further with strong implications for ISM rainfall.

Data Availability Statement

The IMD data set used in the study is available at <https://imd pune.gov.in/lrindex.php> (Pai et al., 2014). The ERA5 data set is available at Hersbach et al. (2023). The CMIP 6 data file used to generate Figure 1c is available at <https://interactive-atlas.ipcc.ch/> (Iturbide et al., 2021) (also available at Github: <https://github.com/IPCC-WG1/Atlas>). The OAflux data set is available at http://apdrc.soest.hawaii.edu/datadoc/whoi_oaflux.php (Yu & Weller, 2007). The HadISST data set is available at <https://www.metoffice.gov.uk/hadobs/hadisst/data/download.html> (Rayner et al., 2003). The Niño 3.4 index and SAM index are downloaded from https://psl.noaa.gov/gcos_wgsp/Timeseries/Nino34/ (Rayner et al., 2003) and <https://climatedataguide.ucar.edu/climate-data/marshall-southern-annular-mode-sam-index-station-based> (Marshall et al., 2022) respectively. The analyses are performed using Python 3.10.0, which is available at <https://www.python.org/downloads/release/python-3100/>.

Acknowledgments

This work was supported by the Natural Environmental Research Council [Grant NE/S007210/1]. Some of the ideas underpinning this research were the outcome of a symposium held over 23–24 November 2023 at the National Oceanography Centre in Southampton (UK), part of the project TRACING moisture sources of extreme rainfall over India—a tool for Better monsoon pRediction at Synoptic Timescales (TRAC-BRISTI), which was in turn supported by a 2023/24 Global Partnership Award from the University of Southampton. The authors would like to thank Lijo Abraham Joseph, Dr Vishnu S Nair, Dr Simon Josey, Dr Bieito Fernandez Castro, and Sreevastha Golla for helpful discussions. We wish to thank Amrita Anil for their help in drawing the schematic summary (Figure 4c).

References

Bhowmick, M., Mishra, S. K., Kravitz, B., Sahany, S., & Salunke, P. (2021). Response of the Indian summer monsoon to global warming, solar geoengineering and its termination. *Scientific Reports*, *11*(1), 9791. <https://doi.org/10.1038/s41598-021-89249-6>

Birner, T., Davis, S. M., & Seidel, D. J. (2014). The changing width of Earth's tropical belt. *Physics Today*, *67*(12), 38–44. <https://doi.org/10.1063/PT.3.2620>

D'Agostino, R., Lionello, P., Adam, O., & Schneider, T. (2017). Factors controlling Hadley circulation changes from the Last Glacial Maximum to the end of the 21st century. *Geophysical Research Letters*, *44*(16), 8585–8591. <https://doi.org/10.1002/2017GL074533>

Dey, D., & Döös, K. (2019). The coupled ocean–atmosphere hydrologic cycle. *Tellus, Series A: Dynamic Meteorology and Oceanography*, *71*(1), 1650413. <https://doi.org/10.1080/16000870.2019.1650413>

Dey, D., & Döös, K. (2021). Tracing the origin of the south Asian summer monsoon precipitation and its variability using a Novel Lagrangian framework. *Journal of Climate*, *34*(21), 8655–8668. <https://doi.org/10.1175/JCLI-D-20-0967.1>

Fogt, R. L., & Marshall, G. J. (2020). The southern Annular Mode: Variability, trends, and climate impacts across the southern hemisphere. *Wiley Interdisciplinary Reviews: Climate Change*, *11*(4). <https://doi.org/10.1002/wcc.652>

Gadgil, S. (2018). The monsoon system: Land–sea breeze or the ITCZ? *Journal of Earth System Science*, *127*(1), 1. <https://doi.org/10.1007/s12040-017-0916-x>

Gadgil, S., & Gadgil, S. (2006). The Indian monsoon, GDP and agriculture. *Economic and Political Weekly*(November 25).

Grise, K. M., & Davis, S. M. (2020). Hadley cell expansion in CMIP6 models. *Atmospheric Chemistry and Physics*, *20*(9), 5249–5268. <https://doi.org/10.5194/acp-20-5249-2020>

Hari, V., Villarini, G., & Zhang, W. (2020). Early prediction of the Indian summer monsoon rainfall by the Atlantic Meridional Mode. *Climate Dynamics*, *54*(3–4), 2337–2346. <https://doi.org/10.1007/s00382-019-05117-0>

Hersbach, H., Bell, B., Berrisford, P., Biavati, G., Horányi, A., Muñoz Sabater, J., et al. (2023). ERA5 monthly averaged data on pressure levels from 1940 to present. [Dataset]. *Copernicus Climate Change Service (C3S) Climate Data Store (CDS)*. <https://doi.org/10.24381/cds.6860a573>

Hersbach, H., Bell, B., Berrisford, P., Hirahara, S., Horányi, A., Muñoz-Sabater, J., et al. (2020). The ERA5 global reanalysis. *Quarterly Journal of the Royal Meteorological Society*, *146*(730), 1999–2049. <https://doi.org/10.1002/qj.3803>

Hrudya, P. H., Varikoden, H., & Vishnu, R. (2021). A review on the Indian summer monsoon rainfall, variability and its association with ENSO and IOD. *Meteorology and Atmospheric Physics*, *133*(1), 1–14. <https://doi.org/10.1007/s00703-020-00734-5>

Hu, Y., & Fu, Q. (2007). Observed poleward expansion of the Hadley circulation since 1979. *Atmospheric Chemistry and Physics*, *7*(19), 5229–5236. <https://doi.org/10.5194/acp-7-5229-2007>

Iturbide, M., Fernández, J., Gutiérrez, J. M., Bedia, J., Cimadevilla, E., Díez-Sierra, J., et al. (2021). Repository supporting the implementation of FAIR principles in the IPCC-WG1 Atlas. [Software]. <https://doi.org/10.5281/zenodo.3691645>

Katzenberger, A., Schewe, J., Pongratz, J., & Levermann, A. (2021). Robust increase of Indian monsoon rainfall and its variability under future warming in CMIP6 models. *Earth System Dynamics*, *12*(2), 367–386. <https://doi.org/10.5194/esd-12-367-2021>

Li, B., Zhou, L., Qin, J., Zhou, T., Chen, D., Hou, S., & Murtugudde, R. (2023). Middle east warming in spring enhances summer rainfall over Pakistan. *Nature Communications*, *14*(1), 7635. <https://doi.org/10.1038/s41467-023-43463-0>

Lu, J., Vecchi, G. A., & Reichler, T. (2007). Expansion of the Hadley cell under global warming. *Geophysical Research Letters*, *34*(6). <https://doi.org/10.1029/2006GL028443>

Lucas, C., Timbal, B., & Nguyen, H. (2014). The expanding tropics: A critical assessment of the observational and modeling studies. *Wiley Interdisciplinary Reviews: Climate Change*, *5*(1), 89–112. <https://doi.org/10.1002/wcc.251>

Lyon, B., & Barnston, A. G. (2005). ENSO and the spatial extent of interannual precipitation extremes in tropical land areas. *Journal of Climate*, *18*(23), 5095–5109. <https://doi.org/10.1175/JCLI3598.1>

Mahendra, N., Chilukoti, N., & Chowdary, J. S. (2024). The increased summer monsoon rainfall in northwest India: Coupling with the north-western Arabian Sea warming and modulated by the Silk Road pattern since 2000. *Atmospheric Research*, *297*, 107094. <https://doi.org/10.1016/J.ATMOSRES.2023.107094>

National Center for Atmospheric Research Staff. (2022). *The climate data Guide: Marshall southern Annular Mode (SAM) index (Station-based)*. In G. Marshall (Ed.). Retrieved from <https://climatedataguide.ucar.edu/climate-data/marshall-southern-annular-mode-sam-index-station-based>

Pai, D. S., Sridhar, L., Rajeevan, M., Sreejith, O. P., Satbhai, N. S., & Mukhopadhyay, B. (2014). Development of a new high spatial resolution (0.25° × 0.25°) long period (1901–2010) daily gridded rainfall data set over India and its comparison with existing data sets over the region. *Mausam*, *65*(1), 1–18. <https://doi.org/10.54302/mausam.v65i1.851>

Prasanna, V. (2014). Impact of monsoon rainfall on the total foodgrain yield over India. *Journal of Earth System Science*, *123*(5), 1129–1145. <https://doi.org/10.1007/s12040-014-0444-x>

Rai, D., & Raveh-Rubin, S. (2023). Enhancement of Indian summer monsoon rainfall by cross-equatorial dry intrusions. *Npj Climate and Atmospheric Science*, *6*(1), 43. <https://doi.org/10.1038/s41612-023-00374-7>

Rajesh, P. V., & Goswami, B. N. (2023). Climate change and potential demise of the Indian deserts. *Earth's Future*, *11*(8). <https://doi.org/10.1029/2022EF003459>

Rao, S. A., Dhakate, A. R., Saha, S. K., Mahapatra, S., Chaudhari, H. S., Pokhrel, S., & Sahu, S. K. (2012). Why is Indian Ocean warming consistently? *Climatic Change*, *110*(3–4), 709–719. <https://doi.org/10.1007/s10584-011-0121-x>

Rao, S. A., Goswami, B. N., Sahai, A. K., Rajagopal, E. N., Mukhopadhyay, P., Rajeevan, M., et al. (2019). Monsoon mission a targeted activity to improve monsoon prediction across scales. *Bulletin of the American Meteorological Society*, *100*(12), 2509–2532. <https://doi.org/10.1175/BAMS-D-17-0330.1>

Rayner, N. A., Parker, D. E., Horton, E. B., Folland, C. K., Alexander, L. V., Rowell, D. P., et al. (2003). Global analyses of sea surface temperature, sea ice, and night marine air temperature since the late nineteenth century. *Journal of Geophysical Research*, *108*(14). <https://doi.org/10.1029/2002jd002670>

Roxy, M. K., Ghosh, S., Pathak, A., Athulya, R., Mujumdar, M., Murtugudde, R., et al. (2017). A threefold rise in widespread extreme rain events over central India. *Nature Communications*, *8*(1), 708. <https://doi.org/10.1038/s41467-017-00744-9>

Roxy, M. K., Ritika, K., Terray, P., & Masson, S. (2014). The curious case of Indian Ocean warming. *Journal of Climate*, *27*(22), 8501–8509. <https://doi.org/10.1175/JCLI-D-14-00471.1>

Roxy, M. K., Ritika, K., Terray, P., Murtugudde, R., Ashok, K., & Goswami, B. N. (2015). Drying of Indian subcontinent by rapid Indian ocean warming and a weakening land–sea thermal gradient. *Nature Communications*, *6*(1), 7423. <https://doi.org/10.1038/ncomms8423>

Saha, K. R., Mooley, D. A., & Saha, S. (1979). The Indian monsoon and its economic impact. *Geojournal*, *3*(2). <https://doi.org/10.1007/BF00257706>

- Schmidt, D. F., & Grise, K. M. (2017). The response of local precipitation and Sea Level pressure to hadley cell expansion. *Geophysical Research Letters*, *44*(20). <https://doi.org/10.1002/2017GL075380>
- Sharma, S., Ha, K. J., Yamaguchi, R., Rodgers, K. B., Timmermann, A., & Chung, E. S. (2023). Future Indian Ocean warming patterns. *Nature Communications*, *14*(1), 1789. <https://doi.org/10.1038/s41467-023-37435-7>
- Skliris, N., Marsh, R., Haigh, I. D., Wood, M., Hirschi, J., Darby, S., et al. (2022). Drivers of rainfall trends in and around Mainland southeast Asia. *Frontiers in Climate*, *4*. <https://doi.org/10.3389/fclim.2022.926568>
- Staten, P. W., Grise, K. M., Davis, S. M., Karnauskas, K., & Davis, N. (2019). Regional widening of tropical overturning: Forced change, natural variability, and recent trends. *Journal of Geophysical Research: Atmospheres*, *124*(12), 6104–6119. <https://doi.org/10.1029/2018JD030100>
- Swapna, P., Krishnan, R., & Wallace, J. M. (2014). Indian Ocean and monsoon coupled interactions in a warming environment. *Climate Dynamics*, *42*(9–10), 2439–2454. <https://doi.org/10.1007/s00382-013-1787-8>
- Wang, B., Liu, J., Kim, H. J., Webster, P. J., Yim, S. Y., & Xiang, B. (2013). Northern Hemisphere summer monsoon intensified by mega-El Niño/southern oscillation and Atlantic multidecadal oscillation. *Proceedings of the National Academy of Sciences of the United States of America*, *110*(14), 5347–5352. <https://doi.org/10.1073/pnas.1219405110>
- Wang, Y. V., Larsen, T., Lauterbach, S., Andersen, N., Blanz, T., Krebs-Kanzow, U., et al. (2022). Higher sea surface temperature in the Indian ocean during the last interglacial weakened the south Asian monsoon. *Proceedings of the National Academy of Sciences of the United States of America*, *119*(10). <https://doi.org/10.1073/pnas.2107720119>
- Xian, T., Xia, J., Wei, W., Zhang, Z., Wang, R., Wang, L. P., & Ma, Y. F. (2021). Is hadley cell expanding? *Atmosphere*, *12*(12), 1699. <https://doi.org/10.3390/atmos12121699>
- Yadav, R. K. (2024). The recent trends in the Indian summer monsoon rainfall. *Environment, Development and Sustainability*. <https://doi.org/10.1007/s10668-024-04488-7>
- Yadav, R. K., & Roxy, M. K. (2019). On the relationship between north India summer monsoon rainfall and east equatorial Indian Ocean warming. *Global and Planetary Change*, *179*, 23–32. <https://doi.org/10.1016/j.gloplacha.2019.05.001>
- Yu, L., & Weller, R. A. (2007). Objectively analyzed air-sea heat fluxes for the global ice-free oceans (1981-2005). *Bulletin of the American Meteorological Society*, *88*(4), 527–540. <https://doi.org/10.1175/BAMS-88-4-527>